JOURNAL OF CATALYSIS 132, 432–439 (1991)

On the Thermal Stability of Zeolite Beta

SHANG-BIN LIU,*,[1] JIN-FU WU,* LONG-JA MA,* TSENG-CHANG TSAI,† AND IKAI WANG†

*Institute of Atomic and Molecular Sciences, Academia Sinica, P.O. Box 23-166, Taipei, Taiwan 10764; †Department of Chemical Engineering, National Tsing Hua University, Hsingchu, Taiwan 30043, Republic of China

Received March 18, 1991

The thermal stability of zeolite beta has been studied by ^{129}Xe NMR and adsorption isotherm of adsorbed xenon in correlation with data from X-ray diffraction and ^{27}Al magic-angle-spinning NMR experiments. Samples subject to different calcination and dehydration conditions were examined. Minor destruction of the crystalline framework resulting from dealumination processes has been found for samples treated at a temperature as small as 400°C. At higher temperatures, a severe process of dealumination involving the breaking of 12-membered rings leads to the conclusion that the maximum regeneration temperature of zeolite beta lies near 760°C.

INTRODUCTION

Zeolite beta is one of the few high-silica zeolites having a structure of three-dimensional 12-membered rings with stacking disorder (*1–5*). Arising from its highly siliceous nature and large pores, many applications of zeolite beta in aromatic transalkylation (*6–8*) and disproportionation (*9, 10*), aliphatic hydrodewaxing (*11, 12*) and hydroisomerization (*13*), and cracking (*14–16*) have been demonstrated. It is well known that the thermal and hydrothermal stabilities of zeolites increase with their Si/Al ratios; the stability of zeolite beta is therefore crucial for practical applications. In practice, the activity of zeolite, which decreases with increasing time-on-stream, is commonly regenerated by burning its coke deposition at a temperature typically in the range 500–700°C. Perez-Pariente *et al.* (*17, 18*) reported a maximum temperature 550°C of thermal stability much below that for zeolites X, Y, or ZSM-5; such behavior is unexpected in relation to its highly siliceous nature. Moreover, the recent results of Bourgeat-Lami *et al.* (*19, 20*) who found a reversible behavior upon dealumination/realumination have shed further light on the stability of zeolite beta.

As the regeneration temperatures of zeolite catalysts lie typically near 600°C, it is of practical importance to justify further the regeneration temperature of zeolite beta. Another important question to be resolved is the origin of structural instability and the corresponding decrease of crystallinity that may accompany framework dealumination. We here report the use of ^{129}Xe NMR and ^{27}Al magic-angle-spinning (MAS) NMR to investigate the stability of zeolite beta at different temperatures of calcination; the instability of the zeolite framework reflecting the changes of pore structure has been monitored by variations of NMR lineshapes and chemical shifts. The NMR results are also correlated with data from X-ray diffraction and xenon adsorption isotherms.

EXPERIMENTAL

The sample of zeolite beta was synthesized with hydrothermal method according to the procedures of Wadlinger *et al.* (*1*); its chemical composition was 95.7 wt% SiO_2

[1] To whom correspondence should be addressed.

0021-9517/91 $3.00

TABLE 1

Treatment Conditions and Characteristics of Zeolite Beta Samples

Sample	A	B	C	D	E	F
Calcination[a]						
Temperature (°C)	None	None	560	760	900	1000
Dehydration[b]						
Temperature (°C)	200	400	400	400	400	400
Duration (h)	60	15	15	15	15	15

[a] Calcined in dry air at a heating rate 3°C min^{-1}, then maintained at the specified temperature for 6 h.

[b] Dehydrated under 10^{-5} Torr vacuum (1 Torr = 133.3 N · m^{-2}); heating rate 1°C min^{-1}.

and 4.29 wt% Al_2O_3 with 3666 ppm Na and 273 ppm Fe. The above analysis gives a molar ratio SiO_2/Al_2O_3 = 37.9. Samples subjected to different thermal treatments are specified in Table 1.

All samples were first calcined under deep bed configuration, enclosed in 10-mm NMR tubes with vacuum stopcock, then subjected to dehydration. Afterward, xenon adsorption isotherms were measured at room temperature (22°C) by a volumetric method. Before the NMR measurements were taken, gaseous xenon was introduced into the sample tube at a particular equilibrium pressure. Room-temperature ^{129}Xe NMR spectra of adsorbed xenon were obtained on a Bruker MSL-300 spectrometer operating at 83.01 MHz. Typically, 10^2–2×10^5 signal acquisitions were accumulated for each spectrum with a recycle delay 0.2 s between 90° pulses. The ^{129}Xe chemical shift values were referred to that of xenon gas extrapolated to zero pressure using the equation reported by Jameson (*21*) and Jameson *et al.* (*22*).

For X-ray diffraction patterns and ^{27}Al NMR experiments, rehydrated samples were used; these rehydrated zeolite samples were prepared by storing under saturated NaCl solution at room temperature for at least 3 days. The ^{27}Al MAS NMR spectra were recorded at 78.21 MHz using the same NMR spectrometer described above. Samples were enclosed in a 7-mm rotor and a spinning frequency of ca. 5 KHz was used. All ^{27}Al NMR spectra were obtained at room temperature using a single-pulse scheme with a recycle delay of 0.3 s. The ^{27}Al chemical shifts were referred to saturated $AlCl_3$ solution. Powder X-ray powder diffraction measurements were made with an automated Siemens D-500 diffractometer using CuKα radiation; the diffraction profiles were scanned in the ω-2θ mode and in steps of 0.02°.

RESULTS AND DISCUSSION

X-Ray Diffraction

The effects of thermal treatment on X-ray diffraction patterns are presented in Fig. 1(a). The diffractogram shows two major characteristic peaks located at $2\theta \simeq 7.8°$ and 22.6°; the pattern is essentially similar to that found previously (*3*). The appearance of both sharp and broad features in the pattern has been ascribed to structural faulting in zeolite beta (*3*). The existence of stacking faults in zeolite beta therefore precludes the derivation of structural data by conventional methods. Nevertheless, the degree of planar faulting can be gauged by simulation of powder diffraction patterns (*3, 23*).

At a calcination temperature $T_c \geq 560°C$, the peak intensity at $2\theta \simeq 22.6°$ decreased with increasing T_c, where the peak intensity at $2\theta \simeq 7.8°$ remained almost unchanged, indicating a decrease in zeolite crystallinity. At T_c = 1000°C, the sharp peaks disappeared so as to reveal a complete collapse of the structure. Observing a similar behavior, Perez-Pariente *et al.* gave a precursor temperature T_c = 550°C for structural instability of zeolite beta calcined overnight in air (*17*). However, Corma *et al.* independently concluded that zeolite beta remains stable up to T_c = 750°C after 3 h of sample steaming treatment under atmospheric pressure (*16*). The X-ray results in this report therefore confirm that the precursor temperature for structural instability of zeolite beta occurs near T_c = 560°C. However, X-ray diffraction data alone cannot provide insight into the mechanisms of the framework collapse.

^{27}Al NMR Experiments

The room-temperature ^{27}Al MAS NMR spectra of rehydrated zeolite beta samples

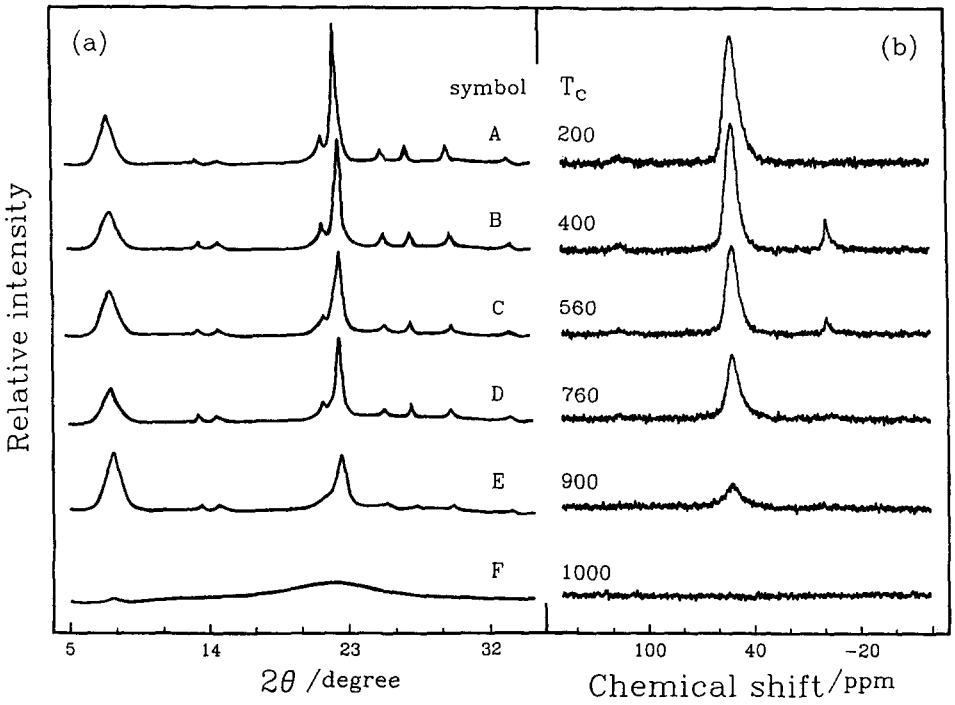

FIG. 1. Variation of (a) X-ray diffraction pattern and (b) ^{27}Al MAS NMR spectrum of zeolite beta with different thermal treatments (Table 1).

are given in Fig. 1(b). The ^{27}Al NMR results are, in general, consistent with the X-ray diffraction data shown in Fig. 1(a). This observation is supported by the decrease of the tetrahedral aluminum peak, chemical shift $\delta \simeq 53$–54 ppm, with increasing T_c. However, the appearance of the octahedral aluminum peak, $\delta \simeq 0$ ppm, at a treatment temperature as small as 400°C is also evident. For $T_c > 400$°C, the octahedral aluminum peak decreased rapidly as T_c was increased indicating that zeolite beta becomes unstable at lower temperatures than previously recognized. At $T_c \geq 1000$°C, both tetrahedral and octahedral aluminum peaks disappeared reflecting the plausible existence of an amorphous phase and the complete destruction of the crystalline framework structure consistent with the X-ray diffraction data shown in Fig. 1(a).

The mechanisms to account for the continuous decrease and subsequent disappearance of both tetrahedral and octahedral aluminum species upon increasing T_c remain the subject of debate. A recent report by Bourgeat-Lami *et al.* observed a 19% decrease in the tetrahedral Al peak while that of the octahedral Al peak remained unchanged after deammoniation of NH_4-β zeolite by calcination at 550°C (*20*). However, the above observations are not compatible with results obtained from this study where a simultaneous decrease in both tetrahedral and octahedral Al peaks upon increasing T_c were evident. Bourgeat-Lami *et al.* (*20*) ascribed the missing Al signal to the formation of "NMR-invisible" Al species associated with Al atoms in asymmetric environments with large quadrupole interactions (*24*). The existence of non-framework Al species has also been found in other zeolites (*25–29*). A subsequent treatment of the sample with acetylacetonate restored most of the Al signal (within the experimental precision of 10%) accompanied by a partial dealumination of framework indicated by a decrease

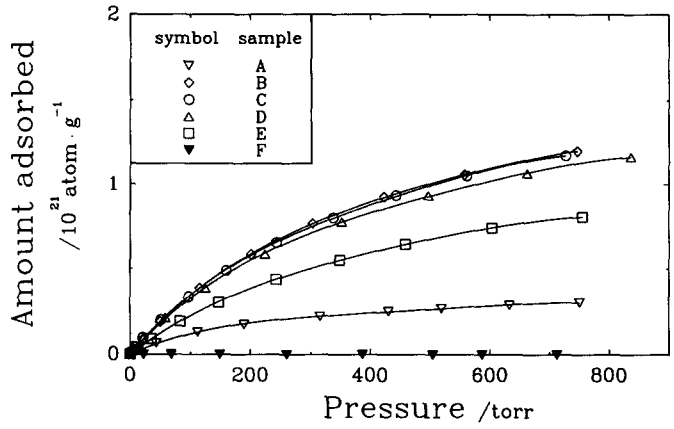

FIG. 2. Xenon adsorption isotherm for samples of zeolite beta with differing thermal treatments (Table 1).

of tetrahedral Al signal and an increase of octahedral Al intensity (*20*). The existence and the nature of NMR-invisible Al species therefore demand future investigation.

For NH_4^+-exchanged zeolite beta, it has been shown that dealumination is more likely to occur in a deep bed calcination and is accompanied by a decrease in the number of hydroxyl groups during calcination treatments (*18*). Although ^{29}Si MAS NMR is useful in probing the framework of zeolites, in the case of zeolite beta ^{29}Si NMR gave ambiguous results (*18, 30*) and the change of the local geometries about the silicon nuclei was found to be negligible with structural reformation (*23*). Therefore, for probing the structural change of zeolite beta, NMR measurements of a non-framework species is desirable. A different approach to this problem has been demonstrated using ^{129}Xe NMR spectroscopy in conjunction with adsorption isotherm measurements of the adsorbed xenon.

^{129}Xe NMR Spectroscopy and Xenon Adsorption Isotherms

^{129}Xe NMR spectroscopy of xenon adsorbed on zeolites, pioneered by Ito and Fraissard (*31*) and by Ripmeester (*32*), has been shown to be a useful probe of its local environment due to its chemical inertness and excellent sensitivity. Owing to its wide range of chemical shift (*21, 22*), ^{129}Xe NMR has been utilized to characterize the void space (*33, 34*) and the structural and chemical properties of zeolites (*31, 35*).

The xenon adsorption isotherms in Fig. 2 show a relatively small capacity of adsorption of sample A, due to the presence of an organic template in the zeolite pores (*17*). Upon dehydration at 400°C (sample B), most template has been removed resulting in a substantial increase of adsorption capacity. For calcined samples, the adsorption capacity decreases with increasing T_c; the dramatic drop in the range 700–900°C is consistent with the X-ray and ^{27}Al NMR results (Fig. 1). Moreover, complete structural collapse at 1000°C is indicated by the lack of adsorption.

The dependence of the ^{129}Xe chemical shift on the density of adsorbed xenon is presented in Fig. 3 with data obtained from dehydrated NaY sample. The measured chemical shift δ of xenon is described as the sum of four terms (*33*):

$$\delta = \delta_0 + \delta_s + \delta_e + \sigma_{xe\text{-}xe} \cdot \rho_{xe},$$

where $\delta_0 = 0$ is the reference, and δ_s corresponds to the shift at zero xenon loading, which represents interactions between xe-

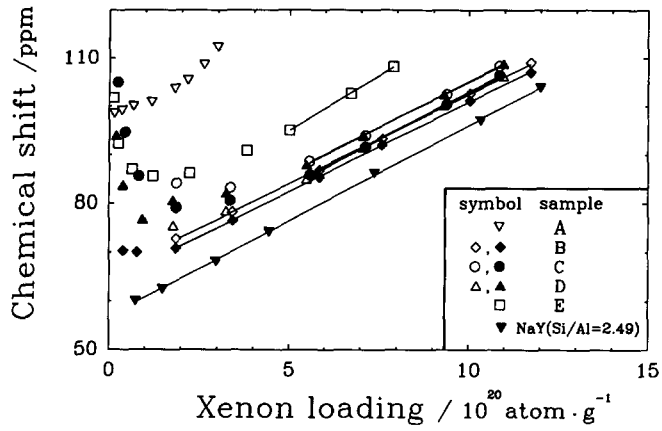

FIG. 3. ^{129}Xe NMR chemical shift (δ) as a function of xenon density (ρ_{xe}) for zeolite beta (Table 1) and dehydrated NaY zeolite.

non atom with the zeolite wall. It has recently been shown that the value of δ_s may be a complicated function of the sorption energy, void space, and temperature (*36*). The term δ_e arises from the "electric effects" caused by the cations or from the presence of strong adsorption sites. The last term, being characteristic of xenon–xenon interactions in which binary collision of xenon atoms dominate, is proportional to density of the adsorbed xenon (ρ_{xe}); the slope of the plot δ vs ρ_{xe} at a sufficiently great density of xenon therefore yields $\sigma_{xe\text{-}xe}$ which may be used to characterize the variation of internal void space of the zeolite.

At 400°C $\leq T_c \leq$ 760°C and for xenon density exceeding ca. 3×10^{20} atom · g^{-1} (Fig. 3), the ^{129}Xe spectra consist of two overlapping peaks, illustrated in Fig. 4 for sample C at various xenon equilibrium pressures. The spacing between the two overlapping peaks is nearly independent of ρ_{xe} and therefore yields nearly equivalent deduced value of $\sigma_{xe\text{-}xe}$. The existence of the two peaks may be attributed to xenon adsorbed in the two slightly different pore systems (*4*) of zeolite beta. The peak at greater chemical shift arises from the smaller 6.5 × 5.6 Å pore system, whereas the peak at smaller chemical shift arises from the other 7.5 × 5.7 Å pore system.

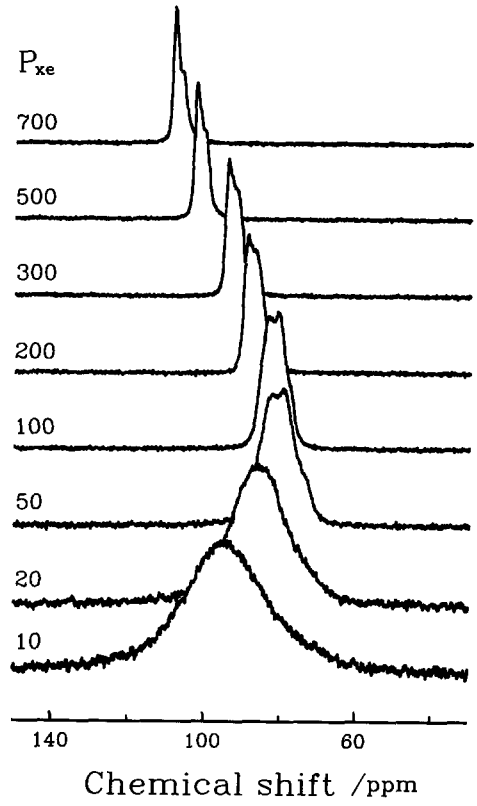

FIG. 4. Comparison of ^{129}Xe NMR spectra of zeolite beta sample C (T_c = 560°C) at various xenon equilibrium pressures (P_{xe}, in Torr).

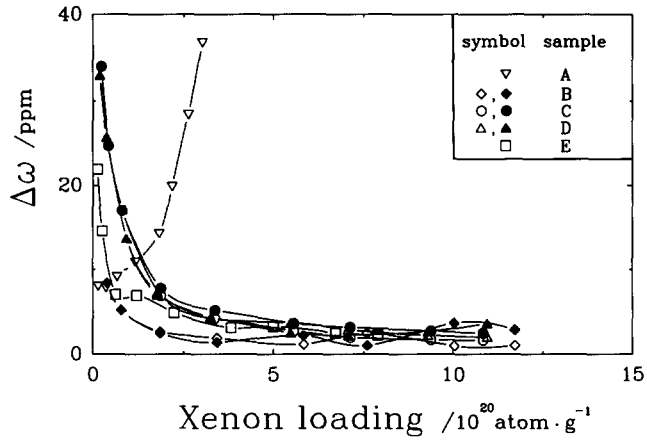

FIG. 5. The variation of zeolite beta (Table 1) ^{129}Xe NMR linewidths ($\Delta\omega$, full width at half maximum) with respect to xenon density ρ_{xe}.

At a sufficiently small density of xenon, a curvature in the density dependence of the chemical shift is evident (Fig. 3). The curvature becomes more severe as T_c increases except for sample A for which the anomalous behavior is mainly due to residual template. The curvature at small xenon density may be due to the presence of defects created by the dealumination processes (*19, 36*) during which extra-framework Al may be formed (*20, 25–29*) or due to the presence of a broad distribution in strength of the sorption sites (*37*). A similar behavior is observed for the observed ^{129}Xe NMR linewidths shown in Fig. 5.

Upon increase of $T_c < 760$°C, despite the anomalous behavior at small xenon loadings, both values of δ_s and $\sigma_{xe\text{-}xe}$ remain practically constant upon extrapolation from a large density of xenon. In contrast, in the same regime, both the slight reduction in adsorption capacity (Fig. 2) and the slight increment of chemical shift at a given xenon loading (Fig. 3) indicate a decrease of pore volume, thus a minor destruction of framework as indicated by ^{27}Al MAS NMR. A similar behavior has been found for the HY zeolite (*38*) for which the authors ascribed the decrease in void volume caused by dealumination processes to be due mainly to the presence of extra-lattice AlO_x groups. Another plausible explanation of these results is that, as xenon is too large to enter satellite cages, the destruction of framework resulting from dealumination occurs mostly in the vicinity of smaller satellite cages, hence only slightly affecting the void volume confined by the 12-membered rings in which xenon atoms reside. In other words, the decrease of pore volume arises from a minor destruction of framework which involve breaking of 4-, 5-, or 6-membered rings. Crystallographic faulting may exist in zeolite beta when treated at elevated temperatures. However, it has been concluded that faulting insignificantly affects the accessible pore volume, but changes only the tortuosity of the pore connectivity along the *c* direction (*3*).

For $T_c > 760$°C, we observed not only an increase of both δ_s and $\sigma_{xe\text{-}xe}$ but also an abrupt decrease of adsorption and a sharp increase of chemical shift at a given ρ_{xe}, thus a drastic decrease of the pore volume confined by the 12-membered rings. The only explanation is a severe dealumination process, which must involve a breaking of the 12-membered rings, as also indicated by the decrease in both the diffraction peak and tetrahedral aluminum peak of the ^{27}Al MAS NMR resonance.

CONCLUSIONS

In summary, the thermal stability of zeolite beta has been studied by the combined methods of ^{129}Xe NMR and adsorption isotherms of adsorbed xenon. Results obtained from the combined methods correlate well with data from X-ray diffraction and ^{27}Al MAS NMR experiments.

For $T_c < 760°C$, minor destruction of the crystalline framework resulting from dealumination processes leads to a slight decrease in pore volume. This behavior is proposed to be caused either by faulting or by dealumination processes that involve breaking of 4-, 5-, or 6-membered rings. For $T_c > 760°C$, a severe process of dealumination involving breaking 12-membered rings that led to a drastic decrease of pore volume has been proposed. The maximum regeneration temperature of zeolite beta therefore lies near 760°C.

We have demonstrated that ^{129}Xe NMR spectroscopy in correlation with other techniques provides valuable structural information about zeolites, especially about zeolites with structural disorder for which this information may not be obtained by any single conventional technique such as X-ray diffraction.

REFERENCES

1. Wadlinger, R. L., Kerr, G. T., and Rosinski, E. J., US Pat. 3,308,069 (1967).
2. Lok, B. M., Cannan, T. R., and Messina, C. A., *Zeolites* **3,** 282 (1983).
3. Newsam, J. M., Treacy, M. M. J., Koetsier, W. T., and De Gruyter, C. B., *Proc. R. Soc. London Ser. A* **420,** 375 (1988).
4. Treacy, M. M. J., and Newsam, J. M., *Nature (London)* **332,** 249 (1988).
5. Higgins, J. B., LaPierre, R. B., Schlenker, J. L., Rohrman, A. C., Wood, J. D., Kerr, G. T., and Rohrbaugh, W. J., *Zeolites* **8,** 446 (1988).
6. Young, L. B., Eur. Pat. 30,084 (1981).
7. Wang, I., Tsai, T. C., and Huang, S. T., *Ind. Eng. Chem. Res.* **29,** 2005 (1990).
8. Innes, R. A., Zones, S. I., and Nacamuli, G. J., US Pat. 4,891,458 (1990).
9. Ratnasamy, P., Bhat, R. N., Pokhriyal, S. K., Hegde, S. G., and Corma, A., *J. Catal.* **119,** 65 (1989).
10. Tsai, T. C., Ay, C. L., and Wang, I., *Proc. Asian Pacific Confederation Chem. Eng. Congress* (1990).
11. McGuiness, M. P., Mitchell, K. M., and Ware, R. A., U.S. Pat. 4,647,368 (1987).
12. Oleck, S. M., and Wilson, R. C., US Pat. 4,568,655 (1986).
13. LaPierre, R. B., Partridge, R. D., Chen, N. Y., and Wong, S. S., US Pats. 4,501,926 (1985) and 4,518,485 (1985).
14. Kennedy, C. R., and Ware, R. A., Eur. Pat. Appl. 186,447 (1986).
15. Chen, N. Y., Ketkar, A. B., Nace, D. M., Kam, A. Y., Kennedy, C. R., and Ware, R. A., Eur. Pat. Appl. 186,446 (1986).
16. Corma, A., Fornes, V., Monton, J. B., and Orchilles, A. V., *J. Catal.* **107,** 288 (1987).
17. Perez-Pariente, J., Martens, J. A., and Jacobs, P. A., *Appl. Catal.* **31,** 35 (1987).
18. Perez-Pariente, J., Sanz, J., Fornes, V., and Corma, A., *J. Catal.* **124,** 217 (1990).
19. Bourgeat-Lami, E., Massiani, P., Di Renzo, F., Fajula, F., and Des Courieres, T., *Catal. Lett.* **5,** 265 (1990).
20. Bourgeat-Lami, E., Massiani, P., Di Renzo, F., Espiau, P., and Fajula, F., *Appl. Catal.* **72,** 139 (1991).
21. Jameson, C. J., *J. Chem. Phys.* **6,** 5296 (1975).
22. Jameson, A. K., Jameson, C. J., and Gutowsky, H. S., *J. Chem. Phys.* **53,** 2310 (1970).
23. Treacy, M. M. J., Newsam, J. M., and Deem, M. W., *Proc. Mol. Res. Sci. Soc. Symp.* **138,** 497 (1990).
24. Man, P. P., and Klinowski, J., *Chem. Phys. Lett.* **147,** 581 (1988).
25. Grobet, P. J., Geerts, H., Tielen, M., Martens, J. A., and Jacobs, P. A., *Stud. Surf. Sci. Catal.* **46,** 721 (1989).
26. Bosacek, V., and Freude, D., *Stud. Surf. Sci. Catal.* **37,** 231 (1988).
27. Lippmaa, E., Samoson, A., and Magi, M., *J. Am. Chem. Soc.* **108,** 1730 (1980).
28. Samoson, A., Lippmaa, E., Engelhardt, G., Lohse, U., and Jerschkewitz, H. G., *Chem. Phys. Lett.* **134,** 589 (1987).
29. Brunner, E., Ernst, H., Freude, D., Frohlich, T., Hunger, M., and Pfeifer, H., *Stud. Surf. Sci. Catal. A* **49,** 623 (1989).
30. Fyfe, C. A., Strobl, H., Kokotailo, G. T., Pasztor, C. T., Barlow, G. E., and Bradley, S., *Zeolites* **8,** 132 (1988).
31. Ito, T., and Fraissard, J., *J. Chem. Phys.* **76,** 5225 (1982).
32. Ripmeester, J. A., *J. Am. Chem. Soc.* **104,** 289 (1982).
33. Benslama, R., Fraissard, J., Albizane, A., Fajula, F., and Figueras, F., *Zeolites* **8,** 196 (1988) and references therein.

34. Ripmeester, J. A., *J. Magn. Reson.* **56,** 247 (1984).
35. Chmelka, B. F., Pearson, J. G., Liu, S. B., Ryoo, R., de Menorval, L. C., and Pines, A., *J. Phys. Chem.* **95,** 303 (1991) and references therein.
36. Ripmeester, J. A., and Ratcliffe, C. I., *J. Phys. Chem.* **94,** 7652 (1990).
37. Cheung, T. P. P., *J. Phys. Chem.* **93,** 7549 (1989).
38. Barrage, M. C., Bonardet, J. L., and Fraissard, J., *Catal. Lett.* **5,** 143 (1990).